Quasi-classical Trajectory Calculations Analyzing the Role of Bending Mode Excitations of Methane in the Cl + CH$_4$ Reaction

J. Sansón, J. C. Corchado, C. Rangel, and J. Espinosa-García*

Departamento de Química Física, Universidad de Extremadura, 06071 Badajoz, Spain

Received: May 9, 2006; In Final Form: June 15, 2006

The effects of the methane torsional (ν_2), umbrella (ν_4), and the combination $\nu_2+\nu_4$ bending mode excitations on the reactivity and dynamics of the gas-phase Cl + CH$_4$ → HCl + CH$_3$ reaction were analyzed. Quasi-classical trajectory (QCT) calculations, including corrections to avoid zero-point energy leakage along the trajectories, were used on an analytical potential energy surface previously developed by our group. With respect to the reactivity, we found that excitation of either bending mode independently gave similar increases in the reactivity, while the increase observed upon excitation of both modes was larger than the sum of the effect of exciting them independently. Both results agree with recent experimental measures. With respect to the dynamics (rotovibrational and angular distributions of the products), the two bending modes and their combination gave very similar pictures, reproducing the experimental behavior. The satisfactory agreement obtained with a great variety of experimental data (always qualitatively acceptable and sometimes even quantitatively) of the present QCT study lends confidence to the potential energy surface constructed by our group.

I. Introduction

The gas-phase Cl + CH$_4$ → HCl + CH$_3$ hydrogen abstraction reaction represents a benchmark system for mode-selective dynamics studies. Experimentally, the state-to-state dynamics study of this reaction is preferred over the similar H + CH$_4$ reaction because in this latter case the dynamics study is very difficult at low energies, due to hot H atoms being produced in the photolysis process, and even in the case of high energies the reaction cross section is very small.

While the effects of stretching mode excitations on polyatomic reactions have been widely studied (for recent publications see, for instance, refs 1 and 2 and references therein), the studies of the effect of nonstretching-activated (bending and torsional) reactions have been few,[3−6] although recently[7−10] they have seen a growth related to the accuracy of experimental techniques. However, these experimental studies present some controversy on the role played by the torsional ($\nu_2 = 1534$ cm^{-1}) and/or umbrella ($\nu_4 = 1369$ cm^{-1}) bending modes of methane on the reactivity and dynamics of this reaction, making it a very interesting subject for theoretical study. While the pioneer work by Kandel and Zare[5] reported that low-energy vibrations (i.e., ν_2 or $\nu_4 = 1$) of methane enhance the reactivity 200 times with respect to the vibrational ground-state methane [CH$_4$ ($\nu = 0$)] at 0.29 eV, a latter study from this same laboratory[9] exciting the CH$_4$ $\nu_2+\nu_4$ modes found only a slight increase of reactivity, 4.5 times with respect to the CH$_4$ ($\nu = 0$) at 0.16 eV. This latter result agrees with another recent experimental study by Zhou et al.[8] which, at a collision energy of 0.20 eV, found that each quantum excitation results in a ~3-fold enhancement in reactivity. This experimental low increase in reactivity for the ν_2 and ν_4 bending mode excited reactants agrees with previous theoretical predictions.[11−15]

Another controversial aspect of the role played by the bending modes is related to the CH$_3$ product vibrational excitation. While

experimentally Zare et al.[5,9] concluded that nearly all the CH$_3$ product is found in its ground state, with only a small amount of umbrella bending (ν_2') excitation, theoretically[13] it was found that the CH$_3$ products are substantially vibrationally excited with $\nu_2' = 1$ being the most probable state. This controversy on the vibrational excitation of the CH$_3$ product would have a great influence on the product scattering distribution.

To shed more light on the issue, and to understand the effects of the torsional (ν_2) and umbrella (ν_4) bending modes, individually and combined, for the gas-phase Cl + CH$_4$ hydrogen abstraction reaction on the reactivity and dynamics (rotovibrational distribution and state-selected differential cross sections of the products), in the present paper we describe an exhaustive quasi-classical trajectory (QCT) study on an analytical potential energy surface, named PES-2005, recently constructed by our group.[15] The article is structured as follows: In section II, we briefly outline the potential energy surface and the computational details of the QCT calculations. In section III, the dynamics results using QCT calculations are presented for the torsional and umbrella bending excitations individually as well as for the simultaneous excitation of the two modes, and they are compared to the little available experimental information. Finally, section IV presents the conclusions.

II. Potential Energy Surface and Computational Details

On previous surfaces from our group for the title reaction[12,14] and with the aim of correcting the observed deficiencies of those surfaces, in 2005 we developed a new PES for this polyatomic reaction,[15] named PES-2005. The functional form and the calibration process are described elsewhere[15] and therefore will not be repeated here.

Because of the large amount of experimental information available for this reaction, this PES-2005 was subjected to a thorough testing of both kinetics and dynamics properties. Thus, from the kinetics point of view, first, the forward and reverse

CH₄ Bending Mode Excitations in the Cl + CH₄ Reaction

J. Phys. Chem. A, Vol. 110, No. 31, 2006 **9569**

thermal rate constants calculated using variational transition-state theory (VTST) with semiclassical transmission coefficients agree with experimental measurements, reproducing the curvature of the Arrhenius plot. Second, we found excellent agreement of the very sensitive $^{12}CH_4/^{13}CH_4$ kinetic isotope effects (KIEs), good agreement for deuterium KIEs, and moderate agreement for the CD_4 KIE. Note that these KIEs are a very sensitive test of features of the new surface, such as barrier height and width, zero-point energy, and tunneling effect.

From the dynamics point of view, an extensive study employing quasi-classical trajectory (QCT) calculations was also performed on this surface, dealing with both ground-state[15] and stretch vibrationally excited[15,16] methane. In general, analyzing the reaction cross section, the rotovibrational excitation of the products, and the state-specific scattering distribution of the products, we found always qualitative agreement with the extensive experimental information, and sometimes even quantitative agreement. In sum, this reasonable agreement lends confidence to this PES-2005 polyatomic surface, although there are some differences which may of course be due to the PES, but also to the known limitations of the QCT method (especially the binning procedure), and/or problems with the way that the experimental data is inverted to obtain scattering angles assuming no methyl excitation.

Quasi-classical trajectory (QCT) calculations[17−19] were carried out using the VENUS96 code,[20] customized to incorporate our analytical PESs. Moreover, it was also modified to compute the vibrational energy in each normal mode to obtain information on the internal vibrational-energy redistribution (IVR). Since VENUS cannot correctly deal with rotating molecules, the normal mode energy calculation is preceded by a rotation of the molecule in order to maintain the orientation of the optimized geometry of the methane molecule for which the normal mode analysis was performed.

The accuracy of the trajectories was checked by the conservation of total energy and total angular momentum. The integration step was 0.1 fs, with an initial separation between the Cl atom and the methane center of mass of 8.5 Å. The rotational energy was thermally sampled at 300 K, with a maximum impact parameter of 3.5 Å. To simulate the experimental conditions,[9] we considered a relative translational energy of 0.159 eV. To compare experimental and theoretical QCT results, for each reaction considered in this work, namely, vibrationally excited CH_4 in ν_2, ν_4, and $\nu_2+\nu_4$, batches of 100000 trajectories were calculated.

To study the IVR in methane we performed batches of 500 nonreactive trajectories of 2 ps. The initial conditions were set so that we ensured that no reaction takes place despite the length of the trajectory. Each set of trajectories was run with excitation of one of the normal modes in methane, and the average energy for each normal mode during the last picosecond was computed for each vibrational state and compared to the average energy obtained from the set of trajectories with no vibrational excitation. The increase in this normal mode average energy was taken as an indication of the internal flow of energy between normal modes in methane. Note that this energy flow occurs before the collision with the Cl atom, so that it is not related to the mode−mode coupling along the reaction path (Coriolis-like terms) that we take as a qualitative indication of the energy flow when a reactive collision occurs.

A serious drawback of the QCT calculations is related to the question of how to handle the quantum mechanical zero-point energy (ZPE) problem in the classical mechanics simulation.[21−27] Many strategies have been proposed to correct this quantum-

TABLE 1: Reactive Cross Section, σ_R,[a] and Reaction Probability, P_R [b]

CH₄ excitation	σ_R	P_R
ν_2	0.54	1.40
ν_4	0.53	1.37
$\nu_2+\nu_4$	1.89	4.90
g.s.[c]	0.28	0.96

	ratios between σ_R		
	σ_2/σ_g	σ_4/σ_g	$\sigma_{2+4}/\sigma_{g.s.}$
QCT	1.91	1.89	6.74
expt	200[d]	200[d]	≥4.5[e]
	3 ± 1[f]	3 ± 1[f]	6 ± 1[f]

[a] In Å²; error bar: ±0.04; b_{max} = 3.5 Å.. [b] Ratio of reactive to total trajectories, in %. [c] Methane vibrational ground-state cross section from ref 15; b_{max} = 3.0 Å. [d] Experimental value from ref 5. [e] Experimental value from ref 9. [f] Experimental value from ref 8.

TABLE 2: Percentage of Product Vibrational Excitation

CH₄ excited mode	HCl ($v' = 0$) QCT	HCl ($v' = 1$) QCT	CH₃ ($v' = 0$) QCT	CH₃ ($\nu_2' = 1$) QCT	CH₃ ($\nu_2' = 1$) expt[c]	CH₃ ($\nu_2' = 2$)[a] QCT	CH₃ (other)[b] QCT
ν_2	100	0	53	35		10	2
ν_4	100	0	55	33		10	2
$\nu_2+\nu_4$	99	1	32	30	21 ± 4	20	18

[a] Another possible excitation is CH₃ ($\nu_4' = 1$). [b] CH₃($\nu_2' \geq 3$), CH₃($\nu_4' \geq 2$), or any combination of ν_2 and ν_4 excitations. [c] Experimental value from ref 9.

dynamics effect, but no completely satisfactory alternatives have emerged. Here, we employed the histogram binning procedure to analyze the reactive trajectories. In our earlier work,[15] five different binning methods were checked to analyze the nascent HCl (v′, j′) product, finding that for the CH₄ vibrationally excited the histogram binning with double ZPE correction (HB-DZPE, which discards all the trajectories that lead to either an HCl with a vibrational energy below its ZPE or to a CH₃ with a vibrational energy below its ZPE) gives better agreement with experiment. Moreover, when the rational rotational numbers (j′) are truncated to their integer part (rounded to the lower integer values instead of to the nearest integer), a narrower rotational distribution and a better agreement with experiment was obtained. Therefore, in the present work we will use the HB-DZPE with the j′ number truncated in the binning procedure.

III. Results and Discussion

First, we begin by analyzing the vibrational frequencies which are excited in this work. The torsional (ν_2) and umbrella (ν_4) bending modes of methane with our PES-2005 surface are, respectively, 1534 and 1369 cm^{-1}, reproducing the experimental values. When the reaction evolves from reactants to products, the "umbrella" mode transforms from ν_4 in CH₄ to ν_2' in CH₃.

Next we analyzed the effect of the vibrational excitation on different dynamics properties: reactivity (section III.A), energy partition in products (section III.B), product rotational distribution (section III.C), and product angular distribution (section III.D).

A. Effect on Reactivity. The QCT reactive cross section, σ_R, for the three bending vibrational excitations considered in this work, namely, ν_2, ν_4, and $\nu_2+\nu_4$, are listed in Table 1.

First, with respect to the methane vibrational ground state, the vibrational excitation of the torsional (ν_2) or umbrella (ν_4) bending modes increases the reactivity by a factor of about 2. This value agrees with recent experimental values, 3 ± 1 (ref 8), and both values therefore strongly contrast with the older
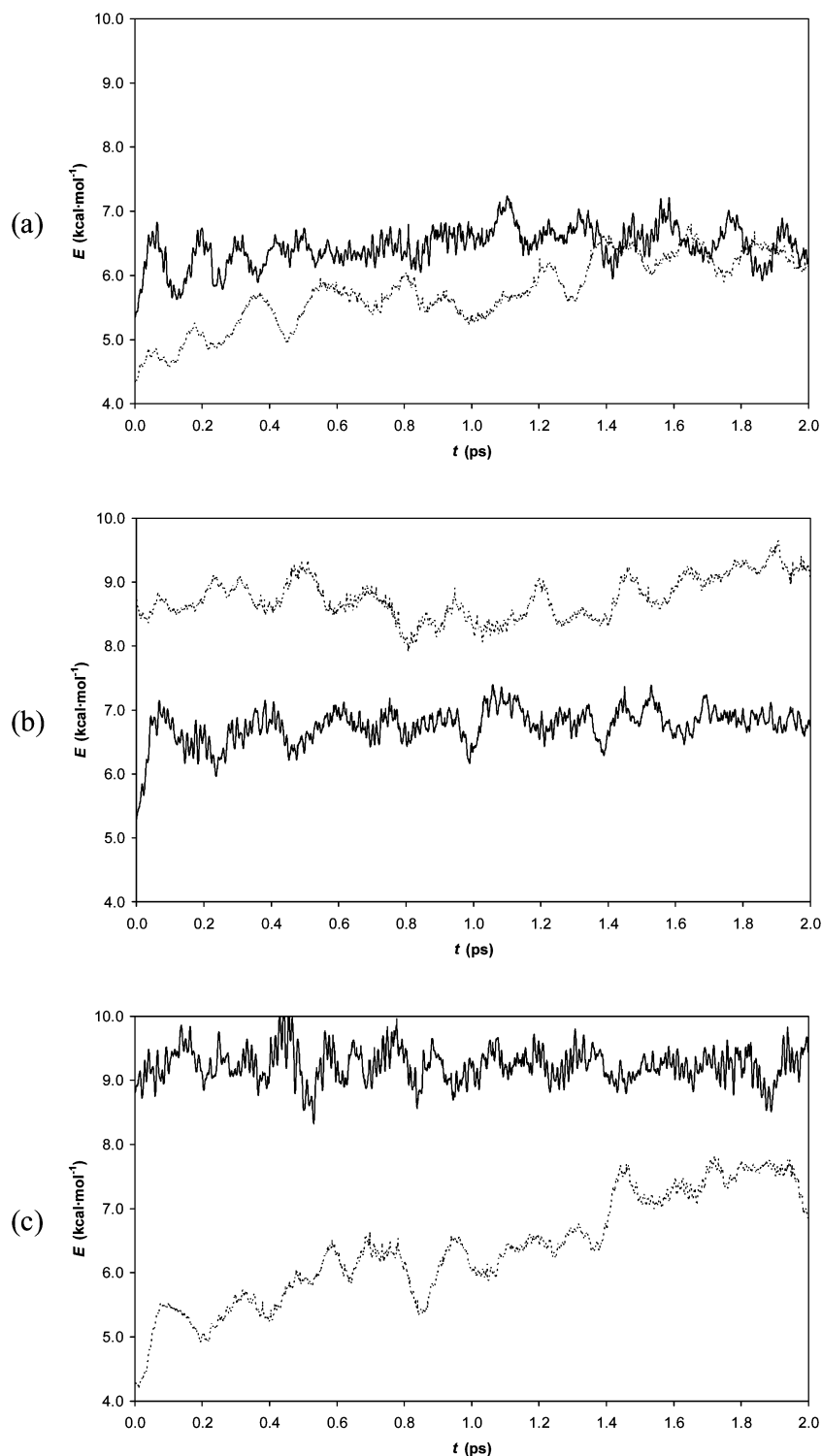
Figure 1. Total energy in the ν_2 and ν_4 modes from trajectories starting from ground-state methane (Panel a), ν_2 excited methane (Panel b), and ν_4 excited methane (Panel c). The dashed line shows the total energy in the three ν_2 modes, the solid line the energy in the two ν_4 modes.

experimental data, 200.[5] Thus, both the torsional and umbrella bending modes have similar effects on the reactivity, which seems reasonable taking into account that excitation by one quantum of each mode requires a similar energy, 4.38 versus 3.91 kcal mol^{-1}. This small difference will be analyzed below. The combined vibrational excitation $\nu_2+\nu_4$ produces an increase of reactivity of 6.74, in excellent agreement with recent experimental measurement, 6 ± 1 (ref 8), and ≥ 4.5 (ref 9).

B. Effect on Energy Partition in Products. A second effect of the CH$_4$ vibrational excitations is on the energy partition in products. For the $\nu_2+\nu_4$ bending excited methane, it was

experimentally found[5,9] that nearly all the CH$_3$ products are formed in the ground state, with only a small amount of umbrella bending ($\nu_{2'}$) excitation.

The percentages of vibrationally excited products obtained from the QCT calculations are listed in Table 2. When the ν_2 or ν_4 bending modes are independently excited, about 50% of the CH$_3$ product is in its ground state, about 35% appears with $\nu_{2'} = 1$, 10% of CH$_3$ has enough energy to be at $\nu_{2'} = 2$ or $\nu_{4'} = 1$, and the rest (2%) can be excited at higher levels. Therefore, independently of which mode is excited, ν_2 or ν_4 in methane, the CH$_3$ product appears vibrationally excited in the umbrella

CH₄ Bending Mode Excitations in the Cl + CH₄ Reaction

J. Phys. Chem. A, Vol. 110, No. 31, 2006 **9571**

TABLE 3: Distribution of the Vibrational Excitation Energy[a]

	normal mode being excited			
	ν_3	ν_1	ν_2	ν_4
ν_3	46%	25%	24%	−10%
ν_1	17%	24%	10%	21%
ν_2	30%	24%	60%	22%
ν_4	7%	27%	6%	67%

[a] When the mode indicated in the header of a column is excited, the percentage of the excitation energy that goes to the mode indicated in the header of a row is listed.

TABLE 4: Maximum Quantum Number That the Mode Indicated in the Header of a Row Can Reach When the Normal Mode Indicated in the Header of the Column Is Excited by One Quantum[a]

	normal mode being excited			
	ν_3	ν_1	ν_2	ν_4
ν_3	0.47	0.25	0.12	−0.05
ν_1	0.18	0.25	0.05	0.10
ν_2	**0.65**	0.48	**0.63**	0.20
ν_4	0.16	**0.61**	0.07	**0.70**

[a] The fractional quantum numbers that exceed 0.5 are in bold.

mode, $\nu_{2'}$. This result is intermediate between the experimental measurement by Kandel and Zare,[5] who observed that the CH₃ product is in $\nu_{2'} = 0$, and the approximate quantum dynamics by Yu and Nyman,[13] who found that the CH₃ product is substantially excited with $\nu_{2'} = 1$ being the most populated state. Therefore, this reaction is not mode-selective, and this behavior is intimately connected with the intramolecular vibrational redistribution (IVR) and will be analyzed below.

The excitation in the $\nu_{2'}$ mode when the ν_4 mode in methane is excited can be explained because, as we found in previous work,[14,15] the ν_4 mode in methane is coupled to the reaction coordinate and adiabatically correlated to the umbrella ($\nu_{2'}$) bending mode of CH₃ product. However, the ν_2 mode in methane is correlated with the $\nu_{4'}$ mode in CH₃. Therefore, with this simple adiabatic selective mode picture, one could a priori expect a difference in energy partition in products between the ν_2 and ν_4 bending modes in methane. We shall return to this subject below.

When both modes are excited, $\nu_2+\nu_4$, more energy is available, and higher vibrational levels of the CH₃ product are excited. Now, only 32% of the CH₃ product is in its vibrational ground state, with 30% excited to $\nu_{2'} = 1$. This last result agrees very well with the single experimental determination,[9] where the excited umbrella bending population found was 21 ± 4%.

With respect to the HCl coproduct, in all cases, ν_2, ν_4, and $\nu_2+\nu_4$, the HCl is formed in its ground state.

To shed more light on the similar effect of the ν_2 and ν_4 excitations on the reactivity and energy partition of the products, we calculated the IVR in methane and the coupling terms between vibrational modes, Bmm′ (Coriolis-type terms).[28] This allows us to analyze the nonadiabatic flow of energy between vibrational modes before the collision and along the reaction path, respectively.

Figure 1 shows the temporal evolution of the energy available on modes ν_2 and ν_4 for the ground state (Panel a) and after excitation of the ν_2 and ν_4 modes (Panels b and c, respectively) averaged over 500 trajectories. Note that the effect of excitation is mostly to shift one of the curves. Thus, the bending mode that we excite in reactants will remain excited until methane collides with the Cl atom, that is, no transfer of energy is observed from ν_2 to ν_4 or vice versa. The increase in the energy of the ν_2 mode along the trajectory can be attributed to its coupling to the ν_3 mode (not shown), whose energy diminishes significantly. Table 3 lists the percentage of the excitation energy that goes to each normal mode upon excitation of either ν_2 or ν_4 averaged over the last picosecond of our simulation and measured with respect to the average energy in a ground-state calculation. For example, when the ν_2 mode was excited by one quantum, only 60% of the excitation energy remains in this mode: 40% is redistributed between the other modes, with 24%, 10%, and 6% going to the ν_3, ν_1, and ν_4 modes, respectively. Table 4 lists the highest fractional quantum number that a mode can reach, according to the average energies listed in Table 3.

Note that the flows between the ν_1 and ν_4 modes and between the ν_3 and ν_2 modes seem to be significant. However, excitation of either the bending or the torsional mode does not involve enough energy to raise the stretching modes to their first excited state. Moreover, the coupling between ν_2 and ν_4 seems to be negligible. Therefore, the IVR upon excitation of either ν_2 or ν_4 will not be important.

Once the reactive collision occurs, the flow of energy between modes can be monitored by the coupling terms Bmm′. Figure 2 shows the coupling matrix for the nine vibrational modes in methane along the reaction path. In this plot, the peaks indicate large coupling between the modes listed on the axes. Hence, in the reactant channel (Panel a), we found some degree of coupling between almost all of the modes. Focusing on the torsional (ν_2) and umbrella (ν_4) bending modes in methane, we found that both modes are strongly coupled, indicating that energy can flow between these bending modes in the entrance channel and therefore that they do not preserve their adiabatic character along the reaction path, that is, the reaction is not vibrationally adiabatic. There is also an important coupling between ν_1 and ν_4 that, as discussed before, cannot have a significant impact on the reactivity of the system since the energy required to excite the ν_1 mode is too high to be provided by the ν_4 excited mode. In the product channel (Panel b), one observes a similar behavior, although with the minor coupling terms vanishing. Therefore, energy flow between the lowest frequency modes of the Cl−CH₄ supermolecule is allowed before and after the transition state.

This result calls into question the simple adiabatic picture of uncoupled normal modes and explains why excitation of either bending mode gives a similar reactivity, $\sigma_2/\sigma_4 = 1.01$, yields CH₃ products excited in the umbrella mode, $\nu_{2'}$, and is not mode-selective, since energy flow between the bending modes is possible both in the reactant and product channels.

C. Effect on Rotational Distribution. For the torsional (ν_2), umbrella (ν_4), and the combination $\nu_2+\nu_4$ excited methane, the QCT rotational population distributions for HCl (v′ = 0, j′) and HCl (v′ = 1, j′) are plotted in Figure 3, together with the only available experimental results for comparison ($\nu_2+\nu_4$). Experimentally,[9] it was found that for the $\nu_2+\nu_4$ excitation the HCl (v′ = 0, j′) state peaks at j′ = 3, while the HCl (v′ = 1, j′) state peaks rotationally hotter at j′ = 4.

Using the HB-DZPE binning procedure for the $\nu_2+\nu_4$ excitation, we reproduce the experimental behavior for the HCl (v′ = 0, j′) state, although the population starts to diminish at slightly lower values of j′ and the distribution is slightly wider. (Note that hot and wide rotational distributions can be an artifact of the QCT calculations.)[29,30] However, we obtain rotational distributions significantly colder than experiment for the HCl (v′ = 1, j′) state. Therefore, contrary to the experiment, we obtain a normal negative correlation of product vibrational and rotational excitations, that is, when the vibrational state is more
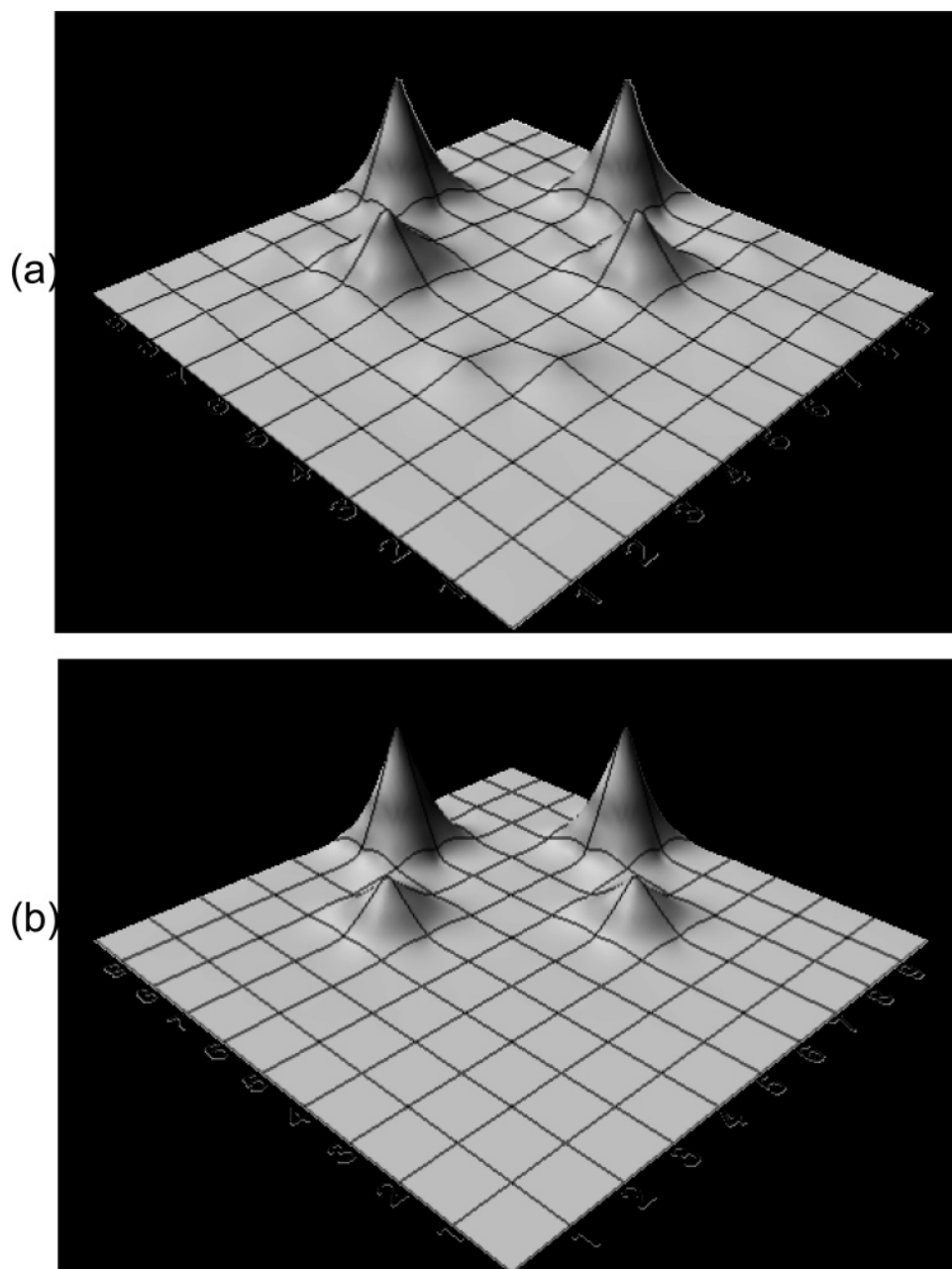
Figure 2. Coriolis-like Bmm′ coupling terms along the reaction path for the nine normal modes in methane. The normal modes are numbered from higher to lower vibrational frequencies. Thus, modes 1, 2, and 3 correspond to ν_3 in methane, mode 4 to ν_1, 5 and 6 to ν_2, and 7, 8, and 9 to ν_4. Panel (a) shows the coupling terms in the reactant channel, while Panel (b) shows the values computed in the product channel. Note that the degeneracy of the modes in methane is broken as the Cl atom approaches it.

excited, the rotational population is lower, which is the usual behavior for direct bimolecular triatomic reactions.

When the bending modes are analyzed independently, that is, ν_2 or ν_4 (Figure 3), only the HCl ($v' = 0$, j') state is populated. In this case, the rotational distribution is similar for both modes, the ν_2 excitation peaking at $j' = 1$ and the ν_4 excitation (with more energy available for the products) peaking at $j' = 3$. Unfortunately, experimental values are not available for comparison, and therefore these QCT theoretical calculations on the PES-2005 surface present an interesting predictive character.

D. Effect on Angular Distribution. For the $\nu_2+\nu_4$ excitation, the angular distributions in terms of the differential cross section (DCS) have been experimentally reported[9] for the states HCl ($v' = 0$, $j' = 6$) and HCl ($v' = 0$, $j' = 10$). Figure 4 plots these experimental DCSs together with our QCT results for comparison. In general, our QCT calculations qualitatively reproduce

the experimental trends (taking the large experimental error bar into account) where the HCl ($v' = 0$) products are side− backward scattered, although our results are more isotropic. Moreover, as j' increases, there is a tendency for the sideward scattering to increase.

The DCSs for the Cl + CH$_4$ ($\nu_2 = 1$) and the Cl + CH$_4$ ($\nu_4 = 1$) reactions independently are plotted in Figure 5, together with experimental[5,8] and other theoretical[13] results for comparison. The two bending excitations show similar tendencies, where the angular distributions of the HCl products show broad side− backward scattering, which is consistent with experimental and previous theoretical results. Our QCT calculations are more isotropic, although in the forward hemisphere they reproduce the trends observed experimentally by Kandel and Zare,[5] while in the backward hemisphere they show a maximum near the
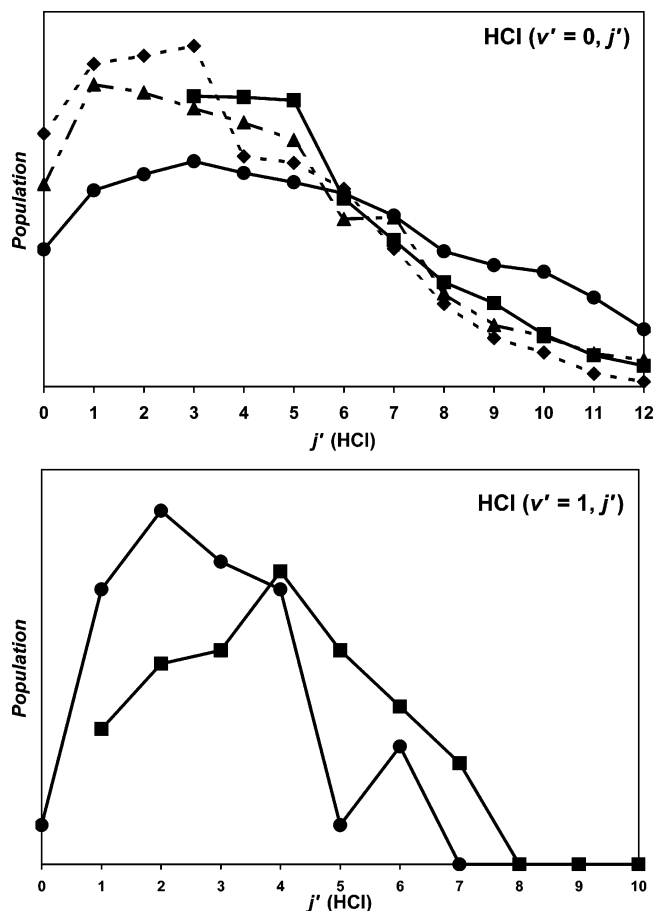
CH$_4$ Bending Mode Excitations in the Cl + CH$_4$ Reaction

J. Phys. Chem. A, Vol. 110, No. 31, 2006 **9573**

Figure 3. Rotational populations of the HCl (v′ = 0, j′) (upper panel) and HCl (v′ = 1, j′) products (lower panel) for the excitation of the $\nu_2+\nu_4$ bending combination in methane. Solid lines with squares are experimental values from ref 9. Solid lines with circles are QCT results from this work. The dashed lines are QCT calculations for the ν_2 excitation (triangles) and for the ν_4 excitation (rhombs). The rotational distributions are normalized so that the area under the common regions is the same.

peak found in the reduced dimensionality quantum scattering calculations of Yu and Nyman.[13]

IV. Conclusions

In this paper we have performed exhaustive QCT calculations in order to analyze the effect of methane vibrational excitations on the reactivity and the dynamics of the reaction with chlorine. With respect to the reactivity, the main conclusions are the following:

1. The torsional (ν_2) and the umbrella (ν_4) bending modes give similar increases in the reactivity with respect to the vibrational ground state, by a factor of about 2, in agreement with recent experimental values, 3 ± 1.

2. The combination of both modes, $\nu_2+\nu_4$, increases reactivity by a factor of 6.74, reproducing recent experimental measurement.

With respect to the dynamics of the excited states, the main conclusions are the following:

1. The two vibrationally excited bending modes, ν_2 and ν_4, give similar rotational and angular distributions of the HCl and the CH$_3$ products.

2. For the $\nu_2+\nu_4$ excitation, the HCl product is found to be vibrationally cold. Moreover, we found a normal negative correlation of product vibrational and rotational excitations, in
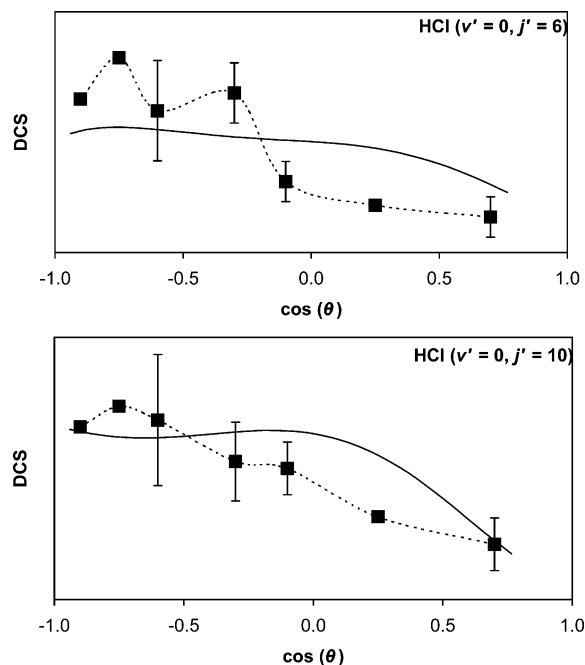

Figure 4. Product angular distributions of the HCl (v′ = 0, j′ = 6) (upper panel) and HCl (v′ = 0, j′ = 10) (lower panel) products for the excitation of the $\nu_2+\nu_4$ bending combination in methane. Dashed lines with squares are experimental values from ref 9. Solid lines are QCT results from this work. The angular distributions are normalized so that the area under the common regions is the same.
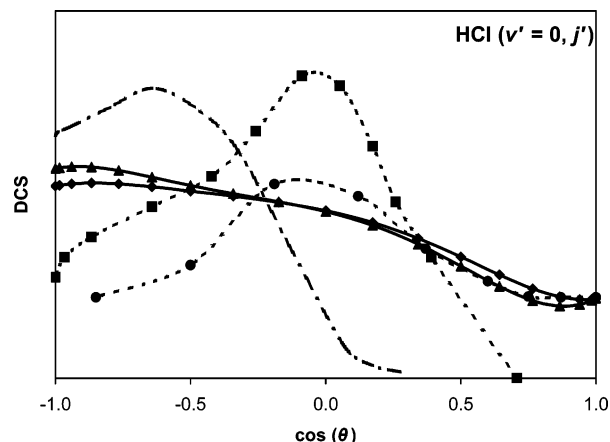

Figure 5. Product angular distributions of the HCl (v′ = 0, j′) products for the independent excitation of the ν_2 and ν_4 bending modes in methane. Dashed lines are experimental values from ref 5 (circles) and from ref 8 (squares). The dash–dot line corresponds to the theoretical values from ref 13. Solid lines are QCT results from this work for the ν_2 (triangles) and ν_4 (rhombs) excitations. The angular distributions are normalized so that the area under the common regions is the same.

agreement with the usual behavior for direct bimolecular reactions, but in contrast with the single experiment.

3. The torsional and umbrella bending modes of methane are strongly coupled along the reaction path, giving rise to a nonadiabatic energy flow between them, and therefore calling into question the simple adiabatic picture.

4. Our QCT calculations on the ν_2, ν_4, and $\nu_2+\nu_4$ excitations qualitatively reproduce the experimental scattering distributions.

References and Notes

(1) Yoon, S.; Henton, S.; Zirkovic, A. N.; Crim, F. F. *J. Chem. Phys.* **2002**, *116*, 10744.

9574 *J. Phys. Chem. A, Vol. 110, No. 31, 2006*

Sansón et al.

(2) Bechtel, H. A.; Camden, J. P.; Brown, D. J. A.; Zare, R. N. *J. Chem. Phys.* **2004**, *120*, 5096.

(3) Sinha, A.; Thoemke, J. D.; Crim, F. F. *J. Chem. Phys.* **1992**, *96*, 372.

(4) Bronikowski, M. J.; Simpson, W. R.; Zare, R. N. *J. Phys. Chem.* **1993**, *97*, 2204.

(5) Kandel, S. A.; Zare, R. N. *J. Chem. Phys.* **1998**, *109*, 9719.

(6) Woods, E., III.; Cheatum, C. M.; Crim, F. F. *J. Chem. Phys.* **1999**, *111*, 5829.

(7) Kim, Z. H.; Alexander, A. J.; Bechtel, H. A.; Zare, R. N. *J. Chem. Phys.* **2001**, *115*, 179.

(8) Zhou, J.; Lin, J. J.; Zhang, B.; Liu, K. *J. Phys. Chem.* **2004**, *108*, 7832.

(9) Kim, Z. H.; Bechtel, H. A.; Camden, J. P.; Zare, R. N. *J. Chem. Phys.* **2005**, *122*, 084303.

(10) Skokov, S.; Bowman, J. M. *J. Chem. Phys.* **2000**, *113*, 4495.

(11) Duncan, W. T.; Truong, T. N. *J. Chem. Phys.* **1995**, *103*, 9642.

(12) Espinosa-Garcia, J.; Corchado, J. C. *J. Chem. Phys.* **1996**, *105*, 3517.

(13) Yu, H.-G.; Nyman, G. *Phys. Chem. Chem. Phys.* **1999**, *1*, 1181.

(14) Corchado, J. C.; Truhlar, D. G.; Espinosa-Garcia, J. *J. Chem. Phys.* **2000**, *112*, 9375.

(15) Rangel, C.; Navarrete, M.; Corchado, J. C.; Espinosa-Garcia, J. *J. Chem. Phys.* **2006**, *124*, 124306.

(16) Sanson, J.; Corchado, J. C.; Rangel, C.; Espinosa-Garcia, J. *J. Chem. Phys.* **2006**, *124*, 074312.

(17) Porter, R. N.; Raff, L. M. In *Dynamics of Molecular Collisions*, Part B; Miller, W. H., Ed.; Plenum Press: New York, 1976.

(18) Truhlar, D. G.; Muckerman, J. T. In *Atom-Molecules Collision Theory*; Bernstein, R. B., Ed.; Plenum Press: New York, 1979.

(19) Raff, L. M.; Thompson, D. L. In *Theory of Chemical Reaction Dynamics*, Vol. 3; Baer, M., Ed.; CRC Press: Boca Raton, 1985.

(20) Hase, W. L.; Duchovic, R. J.; Hu, X.; Komornicki, A.; Lim, K. F.; Lu, D-h.; Peslherbe, G. H.; Swamy, K. N.; Van de Linde, S. R.; Varandas, A. J. C.; Wang, H.; Wolf, R. J. VENUS96: A General Chemical Dynamics Computer Program, *QCPE Bull.* **1996**, *16*, 43.

(21) Truhlar, D. G. *J. Phys. Chem.* **1979**, *83*, 18.

(22) Schatz, G. C. *J. Chem. Phys.* **1983**, *79*, 5386.

(23) Lu, D.-h.; Hase, W. L. *J. Chem. Phys.* **1988**, *89*, 6723.

(24) Varandas, A. J. C. *Chem. Phys. Lett.* **1994**, *225*, 18.

(25) Ben-Nun, M.; Levine, R. D. *J. Chem. Phys.* **1994**, *101*, 8768.

(26) Duchovic, R. J.; Parker, M. A. *J. Phys. Chem.* **2005**, *109*, 5883.

(27) Bonnet, L.; Rayez, J. C. *Chem. Phys. Lett.* **1997**, *277*, 183.

(28) Miller, W. H.; Handy, N. C.; Adams, J. E. *J. Chem. Phys.* **1980**, *72*, 99.

(29) Pomerantz, A. E.; Ausfelder, F.; Zare, R. N.; Althorpe, S. C.; Aoiz, F. J.; Bañares, L.; Castillo, J. F. *J. Chem. Phys.* **2004**, *120*, 3244.

(30) Xiao, T.; Bowman, J.; Duff, J. W.; Braunstein, M.; Ramachandran, B. *J. Chem. Phys.* **2005**, *122*, 014301.